Shape Optimization of Two-layer Acoustical Hoods Using an Artificial Immune Method

Min-Chie CHIU

Department of Mechanical and Automation Engineering, Chung Chou University of Science and Technology
No. 6, Lane 2, Sec.3, Shanchiao Rd., Yuanlin, Changhua 51003, Taiwan, R.O.C.; e-mail: minchie.chiu@msa.hinet.net

Research on acoustical hoods used in industry has been widely discussed; however, the assessment of shape optimization on space-constrained close-fitting acoustic hoods by adjusting design parameters has been neglected. Moreover, the acoustical performance for a one-layer acoustic hood used in a high intensity environment seems to be insufficient. Therefore, an assessment of an optimally shaped acoustical hood with two layers will be proposed. In this paper, a numerical case for depressing the noise level of a piece of equipment by optimally designing a shaped two-layer close-fitting acoustic hood under a constrained space will be introduced. Furthermore, to optimally search for a better designed set for the multi-layer acoustical hood, an artificial immune method (*AIM*) has been adopted as well. Consequently, this paper provides a quick and effective method to reduce equipment noise by optimally designing a shaped multi-layer close-fitting acoustic hood via the *AIM* searching technique.

Keywords: multi-layer; close-fitting acoustical hood; artificial immune method.

Notations

This paper is constructed on the basis of the following notations:

a – the length of the panel,
Ab – the antibody,
abn – the antibody number,
Ag – the antigen,
APC – the antigen appendage cell,
b – the width of the panel,
cn – the clone number,
$cstr$ – the clonal selection threshold,
C_o – the sound speed (m s^{-1}),
d – the distance between the equipment and the hood,
D_i – the panel's complex bulk modulus for the i-th layer of the panel,
div – the diversity,
E – the panel's Young's modulus,
f – the cyclic frequency (Hz),
h – the thickness of the panel,
Ig – the immunoglobulins,
k – the wave number ($= \omega/c_o$),
$maxGen$ – the maximum iteration,
mf – the mutation factor,
$rmtr$ – the remove threshold,
SIL – the sound insertion loss for the acoustical hood (dB),
SPL_T – the total sound pressure level after adding an acoustical hood,
$\rho_o c$ – the acoustic impedance,
η – the panel's internal damping coefficient,
ν – the poison ratio of the panel,
ρ – the panel's density.

1. Introduction

BERANEK, WORK (1949) began the study of acoustical panels using a mass law. Addressing the mechanical resistance, LONDON (1950) proposed the sound transmission loss (*STL*) for a rectangular panel. CROCKER (1994) assessed the sound transmission loss of a resonating/non-resonating panel using a mathematical model. FAHY (1989), BERANEK, VÉR (1992) and KINSLER, FREY (1982) analyzed the sound transmission loss for an infinite acoustical panel. However, it is not easy to evaluate the overall acoustical performance using the *STL*. Additionally, the vibration mode of an acoustical board will be induced by the near-sound-field effect. Therefore, a sound insertion loss (*SIL*) is then considered in evaluating the acoustical efficiency of the acoustic hood Earlier researches (JACKSON, 1962; 1966) indicated that the *SIL* for a close fitting acoustic hood is closely related to the vibration of the vibrating noise source; however, the *SIL* with a negative value is unacceptable. JUNGER (1970) also proposed a theoretical formula for the *SIL*; nevertheless, the accuracy between the theory and the experimental data was inconsistent. Later, the theoretical *SIL* using the plate's vibration model was presented (HINE, 1972). Yet, the accuracy was still

insufficient. Addressing the plate's vibrating effect, a theoretical noise reduction (NR) for a close-fitting acoustic hood was proposed (MORELAND, 1984); but, the formula was valid only for low frequency noise. ROBERTS (1990) also analyzed the SIL of the acoustic hood at the critical frequency. Looking at the effect of the vibrating mode on the hood, the SIL of a close-fitting acoustic hood under both the simple supported boundary condition and the clamped boundary condition was successfully analyzed (OLDHAM, HILARBY, 1991a; 1991b). Results revealed agreement between the accuracy of the theory and the experimental data. Because the constrained problem is mostly concerned with the necessity of operation and maintenance in practical engineering work, there is a growing need to optimize the acoustical performance under a fixed space. However, the research work of shape optimization on a space-constrained close-fitting acoustic hood by adjusting the design parameters, i.e., the panel's damping ratio, the panel's thickness, and the gap between the equipment and the hood has been neglected.

In order to depress efficiently the noise level, a numerical assessment in searching for an optimally shape of a two-layer acoustic hood in conjunction with an artificial immune method (AIM) is proposed. This paper may provide a quick and effective method to reduce equipment noise by optimally designing a shaped two-layer close-fitting acoustic hood.

2. Mathematical models

A two-layer close-fitting acoustic hood made of metal and shown in Fig. 1 is adopted in reducing the equipment' noise. The mathematical model for the acoustic hood is described below.
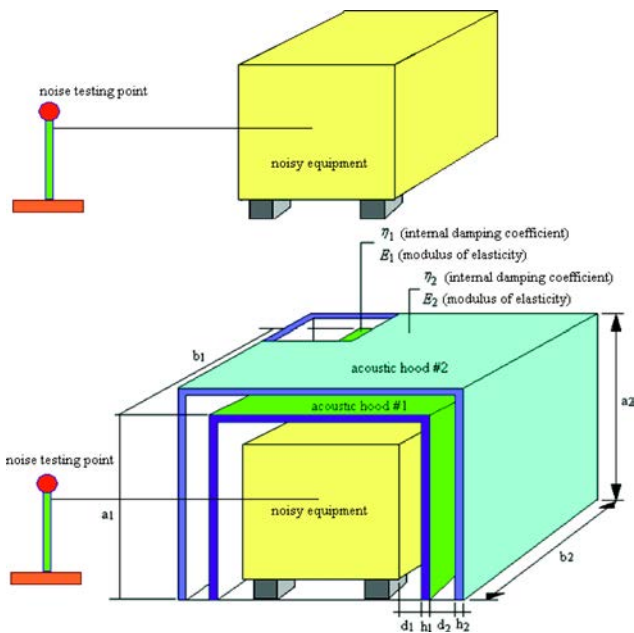

Fig. 1. The noise testing point for a two-layer close-fitting acoustic hood.

2.1. The two-layer close-fitting acoustic hood

According to OLDHAM, HILARBY (1991a; 1991b), for a one-layer close-fitting acoustic hood within a clamped boundary condition, the SIL is

$$SIL(\overline{X}) = 10\log_{10}\left[\left(\cos(kd) + \left(\frac{\pi^2}{4K\omega\rho_o c}\right)\sin(kd)\right)^2\right],$$

$$K = \frac{(1.35)}{\left[3.86D_1\left(\frac{129.6}{a^4} + \frac{78.4}{a^2 b^2} + \frac{129.6}{b^4}\right) - \omega^2\rho h\right]},$$

$$D_1 = \left[\frac{Eh^3}{12(1-\nu^2)}\right](1 + i\eta),$$

$$\overline{X} = (f, h_1, d_1, \eta_1, a, b, E, \rho_1, \nu_1),$$

(1)

where k is the wave number, d is the distance between the equipment and the hood, $\rho_o c$ is the acoustic impedance, E is the panel's Young modulus, D_1 is the panel's complex bulk modulus, a is the length of the panel, b is the width of the panel, η is the panel's internal damping coefficient, h is the thickness of the panel, ν is the poison ratio of the panel, and ρ is the panel's density.

Similarly, for a two-layer close-fitting acoustic hood within a clamped boundary condition, the SIL is

$$SIL(\overline{X}) = 10\log_{10}\left[\left(\cos(kd_1) + \left(\frac{\pi^2}{4K_1\omega\rho_o c}\right)\sin(kd_1)\right)^2 \right.$$
$$\left. \cdot \left(\cos(kd_2) + \left(\frac{\pi^2}{4K_2\omega\rho_o c}\right)\sin(kd_2)\right)^2\right],$$

$$K_1 = \frac{(1.35)}{\left[3.86D_1\left(\frac{129.6}{a_1^4} + \frac{78.4}{a_1^2 b_1^2} + \frac{129.6}{b_1^4}\right) - \omega^2\rho_1 h_1\right]},$$

$$K_2 = \frac{(1.35)}{\left[3.86D_2\left(\frac{129.6}{a_2^4} + \frac{78.4}{a_2^2 b_2^2} + \frac{129.6}{b_2^4}\right) - \omega^2\rho_2 h_2\right]},$$

(2)

$$D_1 = \left[\frac{Eh_1^3}{12(1-\nu_1^2)}\right](1 + i\eta_1),$$

$$D_2 = \left[\frac{Eh_2^3}{12(1-\nu_2^2)}\right](1 + i\eta_2),$$

$$\overline{X} = (f, h_1, d_1, \eta_1, h_2, d_2, \eta_2, a, b, E, \rho_1, \nu_1, \rho_2, \nu_2).$$

2.2. Overall sound pressure level after using an acoustical hood

The silenced octave sound pressure level at the noise testing point shown in Fig. 1 is

$$SPL_i = SPLO_i - SIL_i \tag{3}$$

where $SPLO_i$ is the original SPL at the noise testing point without adding an acoustical hood, and i is the

index of the octave band frequency; SIL_i is the sound insertion loss (SIL) with respect to the relative octave band frequency; SPL_i is the silenced SPL (with an acoustical hood) with respect to the i-th octave band frequency.

Finally, the overall SPL_T silenced by an acoustical hood at a specified location is

$$SPL_T = 10 \log \left\{ \sum_{i=1}^{5} 10^{SPL_i/10} \right\}$$

$$= 10 \log \left\{ \begin{array}{l} 10^{\frac{[SPLO(f=125)-SIL(f=125)]/10}{}} + 10^{\frac{[SPLO(f=250)-SIL(f=250)]/10}{}} \\ + 10^{\frac{[SPLO(f=500)-SIL(f=500)]/10}{}} + 10^{\frac{[SPLO(f=1000)-SIL(f=1000)]/10}{}} \\ + 10^{\frac{[SPLO(f=2000)-SIL(f=2000)]/10}{}} \end{array} \right\}. \quad (4)$$

2.3. Objective function

By using the formulas of Eqs. (2) and (3), the objective function used in the AIM optimization was established

(A) SIL maximization for a one-tone (f) noise

$$OBJ_1 = SIL(f, h_1, d_1, \eta_1, h_2, d_2, \eta_2, \\ a, b, E, \rho_1, \nu_1, \rho_2, \nu_2). \quad (5)$$

(B) SPL_T minimization for a broadband noise

To minimize the overall SPL_T, the objective function is

$$OBJ_2 = SPL_T(h_1, d_1, \eta_1, h_2, d_2, \eta_2, \\ a, b, E, \rho_1, \nu_1, \rho_2, \nu_2). \quad (6)$$

An aluminum-made acoustical hood is selected in the numerical assessment, the related ranges of parameters $(h_1, d_1, \eta_1, h_2, d_2, \eta_2)$ are

$$h_1 : [0.01, 0.02], \qquad h_2 : [0.01, 0.02],$$
$$d_1 : [0.4, 1.0], \qquad d_2 : [0.4, 1.0], \qquad (7)$$
$$\eta_1 : [0.001, 0.1], \qquad \eta_2 : [0.001, 0.1].$$

3. Model check

Before performing the AIM optimal simulation, an accuracy check of the mathematical model on the one-layer close-fitting acoustic hood is performed using the experimental data from BLANKS (1997) As depicted in Fig. 2, the trends of the performance curve with respect to the theoretical and experimental data are relatively similar Therefore, the mathematical model is acceptable.

Consequently, the model linked with the following numerical method is used for optimizing the shape of a two-layer close-fitting acoustic hood in the following section.
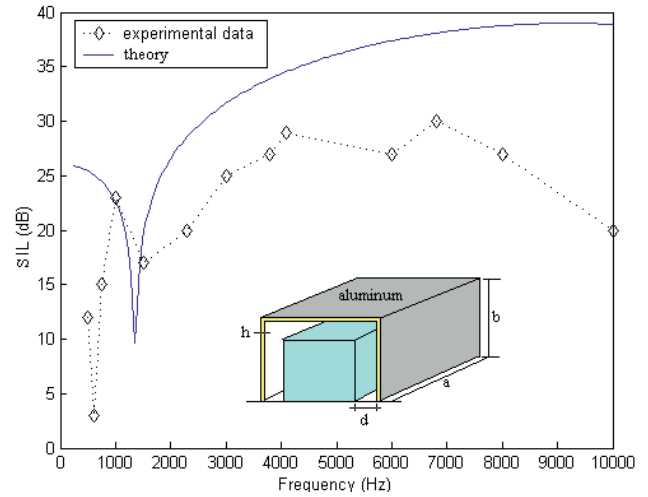

Fig. 2. The performance curve with respect to the theoretical and experimental data $[a = b = 0.293$ (m); $\eta = 0.33$; $d = 0.012$ (m); $h = 0.013$ (m)] (BLANKS, 1997).

4. Case study

An aluminum-made two-layer acoustical hood $(a_1 = b_1 = 0.8$ (M), $E_1 = E_2 = 69 \cdot 10^9$ (Pa), $\nu_1 = \nu_2 = 0.33$, $\rho_1 = \rho_2 = 2700$ kg/m^3) used to depress the noise from a piece of equipment is adopted and shown in Fig. 1. The sound pressure level (SPL) at the noise testing point three meters away from the piece of the equipment is shown in Table 1 where the overall SPL reaches 121.2 dB(A). To eliminate the noise, an aluminum-made acoustical hood with a two-layer close-fitting cover is adopted. To obtain the best acoustical performance within a fixed space, the numerical assessment linked to an AIM optimizer is performed. Before the minimization of a broadband noise is executed, a reliability check of the AIM method by maximization of the SIL at a targeted tone (800 Hz) has been carried out. Moreover, to appreciate the influence of the number of hood layers, two kinds of hoods (a one-layer one and a two-layer one) are accessed and optimized simultaneously.

Table 1. Unsilenced SWL of a root blower inside a duct outlet.

f [Hz]	125	250	500	1 k	2 k	4 k	overall
$SWLO$ [dB(A)]	105	109	119	115	109	105	121.2

5. Artificial immune method

The artificial immune method is originated from an organism's immune system. ISHIDA *et al.* (1998) first published a book related to the artificial immune method. DASGUPTA (1989) and CASTRO and von ZUBEN (1999) started to reorganize the papers, which are related to the artificial immune method. As

indicated in Fig. 3, the antigen appendage cell (APC) will do the antigen appendage reaction when the antigen (Ag) invades the organism; thereafter, the killer T lymphocyte (T-cell) will recognize the Ag and stimulate the B-cell to do clone selection to produce the specific B-cells. The B-cells will transform to the plasma cell and the memory cell when the B-cells become mature. Later, the plasma cell will produce tremendous antibodies (Ab) to extinguish the Ag. The plasma cells will be transformed to the suppressor T cell when all the antigens are extinguished. Consequently the immune reaction for the organism is terminated.
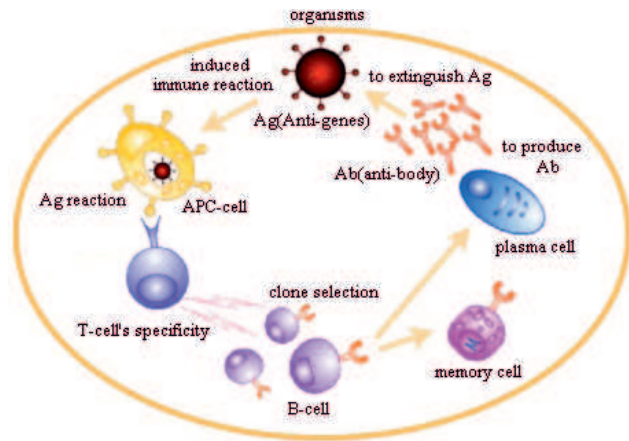

Fig. 3. The immune reaction for an organism (Ku, 2003).

The artificial immune method has the characteristics of the adaptive immune reaction including specificity and adaptability between Ag and Ab, the discrimination of Ag, the clone selection and memory and cytokine of Ab, and the somatic recombination/somatic mutation/regeneration of Ab's genes. Because the artificial immune method is better at both the global and local searching, it has been widely used in various fields to solve the optimization problems such as pattern recognition and classification (CARTER, 2000), engineering search and optimization (MORI *et al.*, 1993; BERSINI, VARELA, 1994; HAJELA *et al.*, 1997), scheduling (FUKUDA *et al.*, 1993; TOMOYUKI, 2003), data mining (KNIGHT, TIMMIS, 2001), and computational security (KEPHART, 1994; KIM, BENTLEY, 1999).

In the whole immune reaction system, the Ab has the recognition specificity of the Ag. The lymphatic system will produce the appropriate Ab to extinguish the pathogen. When using the immune algorithm in the engineering optimization problem, the problem solved will be regarded as the Ag and the solution will be the Ab. Based on the targeted Ag, a better Ag will be searched for step by step. During the immune optimization, the best gene of the Ab will be selected and put into the memory cell for individual generation. Thereafter, the best genes will be kept and used in the next evolution after the screening process in the

memory cell. Each Ab coded by binary bits presents one kind of solution. The string length of the Ab is composed of the design parameters. During the alternation of generations, each Ab has a related affinity with respect to the Ag's solution. During the clone selection process, a specific ratio of Ab having a better affinity will be selected for further reproduction and hypermutation. The best Ag will be selected and put into the memory cell. Additionally, the best gene will be screened from the memory cell and will be randomly selected again to generate the next generation of new Abs using a variety of the gene's heavy chains, the change of gene segment, the transposition of the front/back gene, and the gene mutation. The flow diagram of the artificial immune method is shown in Fig. 4. As indicated in Fig. 4, the operation will be repeated until the integrated iteration reaches a maximal iteration preset in the program. For the single OBJ optimization problem, the mathematical optimization model is

$$Ab = \overline{X} = (x_1, x_2, x_3, ..., x_N), \tag{8}$$

$$Ag = OBJ, \tag{9}$$

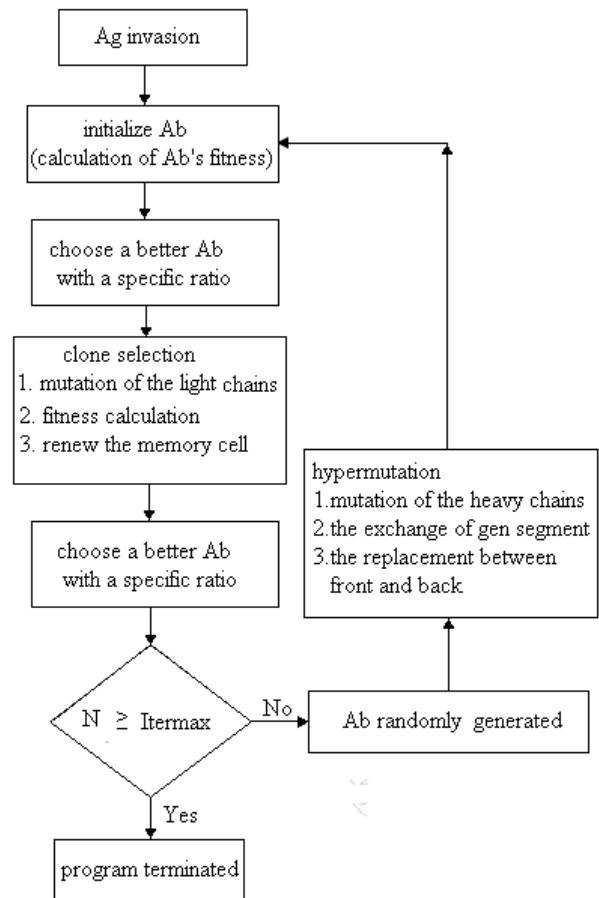$$AbAg = OBJ(\overline{X}), \tag{10}$$

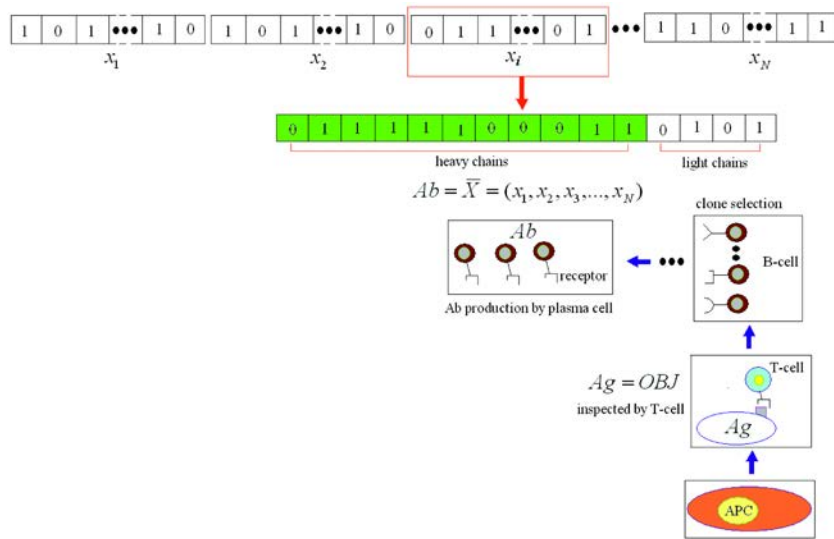Fig. 4. The flow diagram of the artificial immune method.

Fig. 5. The relationship between the immune method and the mathematical optimization model.

where Ab is the anti-body, x_N is the N-th design parameter, and Ag is the anti-gene, $AbAg$ is the affinity between the Ab and Ag. The relationship mentioned above is shown in Fig. 5. To optimally assess the shape of two-layer acoustic hood, the selection of appropriate AIM parameters such as the abn (antibody number), the cn (clone number), the $maxGen$ (max iteration), the mf (mutation Factor), the $rmtr$ (remove threshold), the $cstr$ (clonal selection threshold), and the div (diversity) is essential (KU, 2003).

6. Results and discussion

The accuracy of the AIM optimization depends on the abn, cn, $maxGen$, mf, $rmtr$, $cstr$, and div. To investigate the influences of the above AIM's control pa-

rameter the assessed ranges of the AIM parameters are

$$abn = (10, 30, 50); \qquad cn = (5, 10, 20);$$
$$maxGen = (10, 20, 30); \qquad mf = (30, 50, 80);$$
$$rmtr = (0.05, 0.1, 0.2); \quad cstr = (0.005, 0.01, 0.02);$$
$$div = (0.1, 0.3, 0.5).$$

6.1. Results

A. Pure tone noise optimization

By using Eq. (5), the maximization of the SIL with respect to a two-layer close-fitting acoustical hood at the specified pure tone (800 Hz) was performed first. As indicated in Table 2, fifteen sets of the AIM param-

Table 2. Optimal result of a two-layer close-fitting acoustical hood with respect to various AIM parameters at targeted tones of 800 Hz.

Item	AIM parameter							Design parameters						SIL
	abn	cn	$maxGen$	mf	$rmtr$	$cstr$	div	h_1 [m]	d_1 [m]	η_1	h_2 [m]	d_2 [m]	η_2	
1	10	5	20	30	0.2	0.01	0.5	0.014033	0.63015	0.052384	0.012602	0.63832	0.064518	57.7
2	30	5	20	30	0.2	0.01	0.5	0.012617	0.63785	0.070006	0.017065	0.99757	0.096424	68.1
3	50	5	20	30	0.2	0.01	0.5	0.015452	0.85682	0.064976	0.019428	0.63495	0.067477	72.5
4	50	10	20	30	0.2	0.01	0.5	0.018895	0.63574	0.093396	0.011489	0.65673	0.062876	75.5
5	50	20	20	30	0.2	0.01	0.5	0.012527	0.84595	0.09478	0.014814	0.618	0.061297	81.5
6	50	20	10	30	0.2	0.01	0.5	181.9	0.84686	0.06558	0.012167	0.87314	0.053146	82.2
7	50	20	30	30	0.2	0.01	0.5	0.015627	0.86124	0.081168	0.017345	0.86086	0.055864	88.3
8	50	20	30	80	0.2	0.01	0.5	0.011714	0.62596	0.069549	0.010007	0.95446	0.087702	97.3
9	50	20	30	50	0.2	0.01	0.5	0.011567	0.72771	0.053541	0.011862	0.86506	0.081255	100.6
10	50	20	30	50	0.1	0.01	0.5	0.010499	0.61794	0.053804	0.018962	0.54962	0.082531	106.1
11	50	20	30	50	0.05	0.01	0.5	0.017153	0.77562	0.0721	0.010168	0.80791	0.099968	110.5
12	50	20	30	50	0.05	0.005	0.5	0.013298	0.55348	0.056405	0.010093	0.52923	0.080254	113.4
13	50	20	30	50	0.05	0.02	0.5	0.019521	0.74644	0.05211	0.014598	0.81177	0.050382	115
14	50	20	30	50	0.05	0.02	0.3	0.01651	0.74132	0.096989	0.012308	0.95382	0.073184	117.4
15	50	20	30	50	0.05	0.02	0.1	0.01756	0.76061	0.092359	0.017962	0.72055	0.058737	120.5

eters are tried in the acoustical hood's optimization. Obviously, the optimal design data can be obtained from the last set of the *AIM* parameters at (*abn, cn, maxGen, mf, rmtr, cstr, div*). Table 2 reveals that the optimal design data is obtained in the last set of the *AIM* parameters at ($abn = 50$, $cn = 20$, $maxGen = 30$, $mf = 50$, $rmtr = 0.05$, $cstr = 0.02$, $div = 0.1$). Using the optimal design data in the theoretical calculation, the resultant curves of the *SIL* with respect to various *AIM* parameters (*abn, cn, maxGen, mf, rmtr, cstr, div*) are depicted in Figs. 6–8. As revealed in Fig. 8, the *SIL* is precisely maximized at the desired frequency.

Moreover, to realize the influence of the acoustical performance with respect to the number of hood layers, a one-layer acoustical hood is also optimally assessed. As indicated in Fig. 9, the acoustical performance of a two-layer acoustical hood is much better than that of a one-layer acoustical hood.
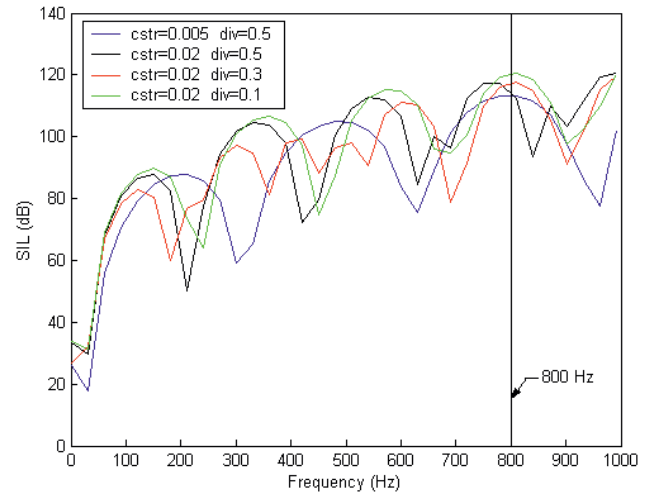

Fig. 8. The *SIL* with respect to frequencies at various *AIM* parameters (*cstr, iter*) (targeted tone: 800 Hz).
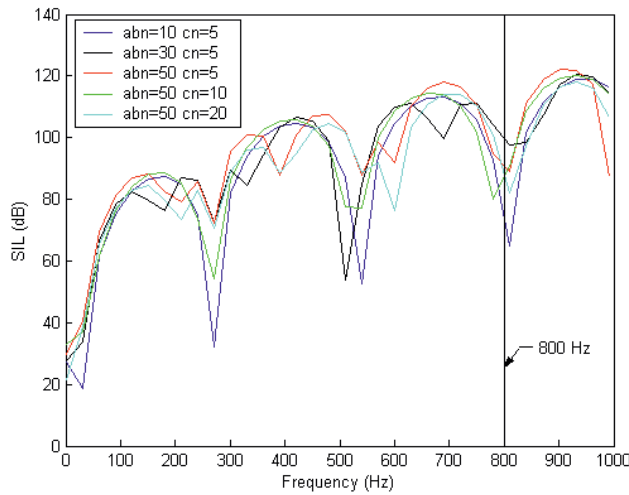

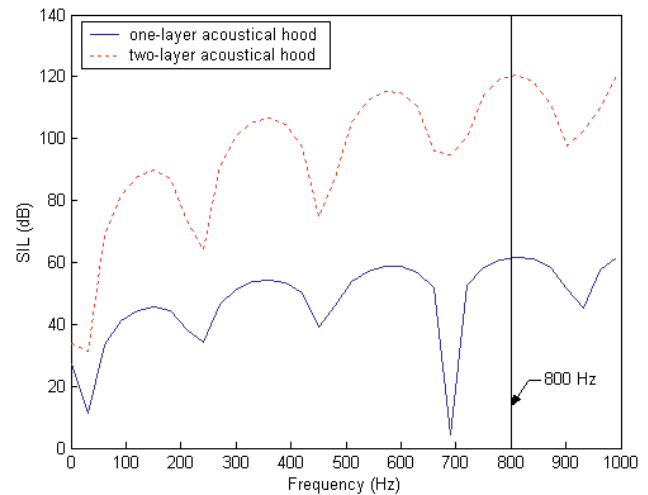Fig. 6. The *SIL* with respect to frequencies at various *AIM* parameters (*abn, cn*) (targeted tone: 800 Hz).

Fig. 9. The optimal *SIL* curves with respect to one-layer and two-layer acoustical hood [optimal design set of a one-layer acoustical hood is ($d_1 = 0.019781$; $h_1 = 0.73809$; η_1)] (targeted tone: 800 Hz).

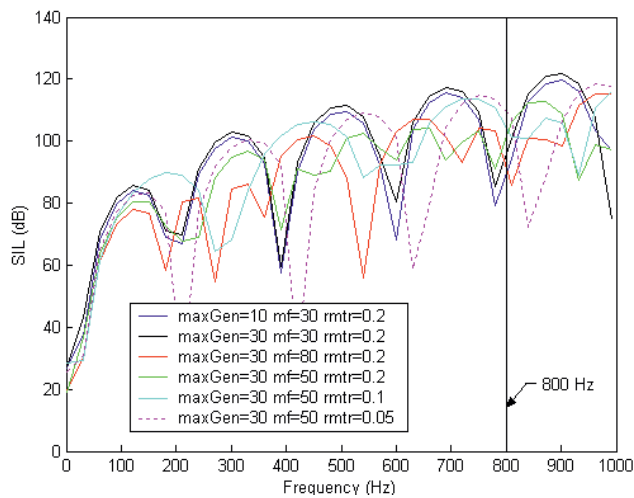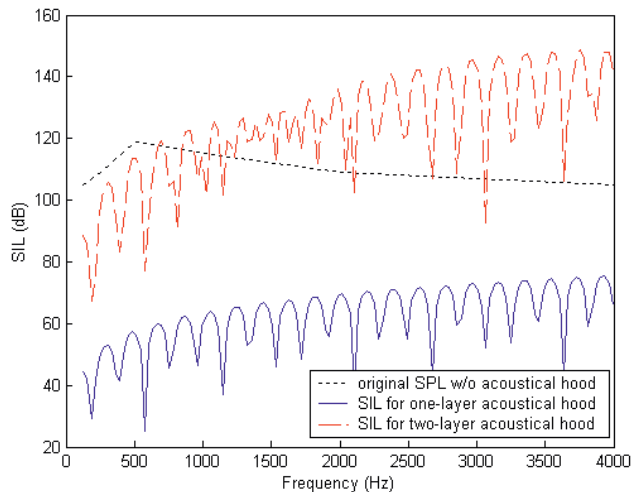### B. Broadband noise optimization

Using the formulas of Eq. (6) and the *AIM* parameters of ($abn = 50$, $cn = 20$, $maxGen = 30$, $mf = 50$, $rmtr = 0.05$, $cstr = 0.02$, $div = 0.1$), the minimization of the sound pressure level of the noise emitted at the noise testing point is performed. Moreover, to realize the influence of the acoustical performance with respect to the number of hood layers, a one-layer acoustical hood is also optimally assessed. As indicated in Table 3, the SPL_T for the two-layer acoustical hood at the noise testing point can reach 18 dB(A); however, the SPL_T for the one-layer acoustical hood at the noise testing point is 65.8 dB(A). Using these optimal design data in the theoretical calculation, the resultant curve of the SPL_T with respect to the original *SPL* are plotted in Fig. 10.

Fig. 7. The *SIL* with respect to frequencies at various *AIM* parameters (*maxGen, mf, rmtr*) (targeted tone: 800 Hz).

Table 3. Optimal result for two kinds of close-fitting acoustical hoods (a one-layer and a two-layer) with respect to various *AIM* parameters (broadband noise).

Item	Design parameters						SPL_T dB(A)
	h_1 [m]	d_1 [m]	η_1	h_2 [m]	d_2 [m]	η_2	
A one-layer acoustical hood	0.02	0.88897	0.098412				65.8
A two-layer acoustical hood	0.019582	0.83245	0.056577	0.019524	0.88876	0.05795	18.0

Fig. 10. Comparison of the original *SPL* and an optimal *SIL* for a two-layer close-fitting acoustic hood (broadband noise).

6.2. Discussion

To achieve a sufficient optimization, the selection of the appropriate *AIM* parameter set is essential. As indicated in Table 2 and Figs. 6–8, the best *AIM* set with respect to a one-layer close-fitting acoustical hood at the targeted pure tone noise of 800 Hz has been shown. Figure 8 reveals that the predicted maximal value of the *SIL* is precisely located at the desired frequency. Therefore, using the *AIM* optimization in finding a better design solution is reliable; moreover, the investigation of the influence of the number of hood layers (one-layer and two-layer) has been shown in Fig. 9. Figure 9 reveals that when dealing with the pure tone noise, the acoustical performance for a two-layer acoustical hood is superior to that of the one-layer acoustical hood.

Furthermore, the investigations in dealing with the broadband noise using both the one-layer and two-layer close-fitting acoustical hoods have been shown in Table 3 and Fig. 10. As indicated in Table 3, the overall sound insertion loss of the optimally shaped acoustical hoods with respect to two kinds of acoustical hoods (one-layer and two-layer) reached 55.4 dB(A) and 103.2 dB(A). As indicated in Fig. 10, the *SIL* curve of the two-layer acoustical hood can provide a more efficient noise reduction in lowering the whole *SPL* curve.

7. Conclusion

It has been shown that an *AIM* can be used in the optimization of acoustical hood shape. The *AIM* parameters such as the *abn*, the *cn*, the *maxGen*, the *mf*, the *rmtr*, the *cstr*, and the *div* play essential roles in the *AIM* optimization. The higher *abn*, *cn*, and *max-Gen* will result in a better solution. As can be seen that using the best *AIM* set, the predicted maximal value of the *SIL* can be precisely located at the desired frequency.

Moreover, in dealing with the broadband noise, the overall sound insertion loss of the optimally shaped acoustical hoods with respect to two kinds of acoustical hoods (one-layer and two-layer) achieved 55.4 dB(A) and 103.2 dB(A). Observably, the *SIL* curve of the two-layer acoustical hood can provide a more effective noise reduction in depressing the whole *SPL* curve.

Consequently, this study could provide an effective and quick method for optimally designing the shape of multi-layer acoustical hoods.

Acknowledgment

References

1. BERANEK L.L., WORK G.A. (1949), *Sound transmission through multiple structures containing flexible blankets,* J. Acoust. Soc. Am., **7**, 419.

2. BERANEK L.L., VÉR I.L. (1992), *Noise and vibration control engineering,* John Wiley and Sons, New York.

3. BERSINI H., VARELA F.J. (1994), *The immune learning mechanisms: reinforcement, Recruitment and their applications,* [in:] Computing with Biological Metaphors, Paton R. [Ed.], Chapman and Hall.

4. BLANKS J.E. (1997), *Optimal Design of an Enclosure for a Portable Generator,* Unpublished Master Thesis, Virginia Polytechnic Institute and State University.

5. CARTER J.H. (2000), *The immune system as a model for pattern recognition and classification,* Journal of the American Medical Information Association, **7**, 1, 28–41.

6. CROCKER M.J. (1994), *A system approach to the transmission of sound and vibration through structures,* Noise-Con 94, 525–533.

7. Dasgupta D. (1999), *Artificial immune systems and their applications*, Springer-Verlag.

8. de Castro L.N., von Zuben F.J. (1999), *Artificial immune systems: part I-basic theory and applications,* Technical Report, **TR-DCA01/99**.

9. Fahy F. (1989), *Sound and structural vibration*, Academic Press, San Diego, Ca.

10. Fukuda T., Mori M., Tsukiyama M. (1993), *Immune network genetic algorithm for adaptive production scheduling*, Proceeding of the 15th IFAC World Congress, **3**, 57–60.

11. Hajela P., Yoo J., Lee J. (1997), *GA based simulation of immune networks-application in structural optimization*, Engineering Optimization, **29**, 131–149.

12. Hine M.J. (1972), *Acoustic hood design in theory and practice*, Noise-Con, 72, 278–281.

13. Ishida Y., Hirayama H., Fujita H., Ishiguro A., Mori K. (1998), *Immunity-based systems-intelligent system by artificial immune systems* [in Japanese], Corona Pub. Co. Japan.

14. Jackson R.S. (1962), *The performance of acoustic hoods at low frequencies*, Acustics, **12**, 139–152.

15. Jackson R.S. (1966), *Some aspects of acoustic hoods*, Journal of Sound and Vibration, **3**, 82–94.

16. Junger M.C. (1970), *Sound through an elastic enclosure acoustically coupled to a noise source*, ASME Paper No – WA/DE – 12.

17. Kephart J.O. (1994), *A biological inspired immune system for computers*, [in:] Artificial Life IV Proceeding of the Fourth International Workshop on the Synthesis and Simulation of Living Systems, Brooks R.A., Maes P. [Eds.], MIT press.

18. Kim J., Bentley P. (1999), *Negative selection and niching by an artificial immune system for network in-* strusion Detection, Proceeding of Genetic and Evolutionary Computation Conference, 149–158.

19. Kinsler L.E., Frey A.R. (1982), *Fundamentals of acoustics*, John Wiley and Sons, New York.

20. Knight T., Timmis J. (2001), *AINE: an immunological approach to data mining*, Proceeding of the IEEE International Conference on Data Mining, 297–304.

21. Ku C.C. (2003), *Multimodal Topology Optimization of Structure Using Distributed Artificial Immune Algorithm*, Unpublished Master Thesis, Department of Mechanical Engineering, Tatung University.

22. London A. (1950), *Transmission of reverberant sound through single wall,* J. Acoust. Soc. Am., **22**, 270–279.

23. Moreland J.B. (1984), *Low frequency noise reduction of acoustic enclosures,* Noise Control Engineering Journal, **23**, 3, 140–149.

24. Mori M., Tsukiyama M., Fukuda T. (1993), *Immune algorithm with searching diversity and its application to allocation problem*, Trans. of Institute of Electrical Engineering of Japan, **113-C**, 10, 872–878.

25. Oldham D.J., Hilarby S.N. (1991a), *The acoustical performance of small close fitting enclosures, part 1: theoretical methods*, Journal of Sound and Vibration, **150**, 261–281.

26. Oldham D.J., Hilarby S.N. (1991b), *The acoustical performance of small close fitting enclosures, part 2: experimental investigation,* Journal of Sound and Vibration, **150**, 283–300.

27. Roberts J. (1990), *The principle of noise control with enclosures*, Journal of Electrical and Electronic Engineering, Australia, **10**, 3, 151–155.

28. Tomoyuki M. (2003), *An application of immune algorithms for job-shop scheduling problems*, Proc. of the 5th International Symposium on Assembly and Task Planning, 146–150.